

## Application of Force Feedback to Heavy Duty Hydraulic Machines

N.R. Parker

S.E. Salcudean

P.D. Lawrence

Dept. of Electrical Engineering, University of B.C., Vancouver, B.C., Canada

### Abstract

*This paper presents a summary of the design and implementation of a force-reflecting controller for conventional heavy duty hydraulic machines. The unsuitability of direct force feedback with rate control has been shown analytically and confirmed on a simulator of a typical hydraulic machine. A novel stiffness control scheme was developed to circumvent this problem and was used successfully in controlling the endpoint force on a CAT 215 log loader to better than 10% of a typical working load. A magnetically levitated wrist was used as a force-reflecting master, while the endpoint forces were obtained from hydraulic cylinder pressures.*

### 1 Introduction

Force feedback can provide useful information to the operator of a teleoperation manipulator. Assembly tasks can usually be completed much faster when the operator has a feel for the forces and torques caused by contact [1]. Other benefits include improved safety and less damage from overstressing the manipulator or materials being handled. The goal of this research is to provide the operators of heavy duty hydraulic machines with these benefits by developing a system that can provide useful force feedback.

Currently, the hydraulic machines in use in the forestry, mining and construction industries provide no force feedback to the operator. The operator controls motion of the machine by manipulating hydraulic valves (either directly or electrically) which in turn control the forces applied to the machine joints. The control system is unilateral, with endpoint forces completely isolated. Machine loading can be determined only by experienced operators relying on such cues as cabin motion and engine audio.

The forest industry uses several types of hydraulic machines in harvesting, processing and transportation. This work concentrates on the control of feller/bunchers which are hydraulic machines based on an excavator frame (Fig. 1). Force feedback in this application could provide the operator with better control when manipulating large trees, better safety through increased awareness of machine tip over, as well as potential for reduced machine wear and wood damage.

Excavators are an excellent target for application of force feedback. This was noticed by both researchers [2] and manufacturers [3].

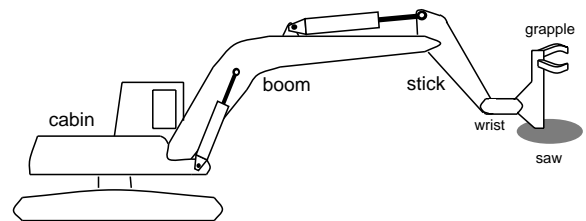


Figure 1 Typical Feller/Buncher

There has been quite a bit of work in force reflecting master/slave manipulators (see, for example [4],[5]). While most early work used kinematically equivalent masters, a generalized master can provide more versatility [6]. In the work presented here, a magnetically levitated master developed and built at UBC [7] along the principles described in [8], will be used.

A summary of system requirements for effective force feedback was made in [9]. It was found that while forces could be felt at relatively high frequencies (up to 3 kHz) the absolute maximum command frequency would be less than 10 Hz. A summary of operator hand modeling can be found in [10], with the primary finding that, while the human arm is an active element, the response is slow enough that it can be effectively modeled as a passive impedance.

The treatment of hydraulic machines as teleoperators has been investigated by Lawrence *et al.* [11]. The addition of coordinated control to such machines was found to be useful in reducing operator training time [12].

A comparison between position and rate control (without force feedback) was done by Kim *et al.* [13]. It was found that position control was better in the ideal case for relatively small manipulator workspaces, though its superiority depends on a fast manipulator. Rate control is more effective for large workspaces and slow manipulators.

This research project has focussed on the addition of useful force feedback to heavy duty hydraulic equipment. A graphical simulator was developed and integrated with a force reflecting joystick. Rather than using kinematic

equivalence, a universal master was used, with the necessary coordinate transformations being processed in software. The force reflecting master was also integrated into a CAT 215 log loader equipped with a coordinated motion controller and endpoint force sensing via main hydraulic pressures. The integrated system was used to successfully control the applied endpoint force of the machine. A novel approach to force feedback which involves controlling the joystick stiffness has been developed. This method shows promise of providing endpoint force feedback while controlling the machine in rate mode.

The remainder of this paper will present the development and results from a real time simulation of a feller/buncher. Some analysis of the addition of force feedback, in particular to systems controlled in rate mode is presented. Finally, the experimental results of a machine implementation of the force feedback controller are given.

## 2 Computer simulation

The goal of this project was the development and implementation of a practical force feedback system on a hydraulic machine, preferably a feller/buncher, using a magnetically levitated joystick as the force reflecting master. To this end, a real time computer simulation was developed to test different control methods (position, rate and hybrid schemes) and different feedback methods (force, force derivative and stiffness). The system consists of the maglev wrist and controller, a dynamic simulation of the endpoint load, and graphic simulation of the operator viewpoint (Fig. 2).

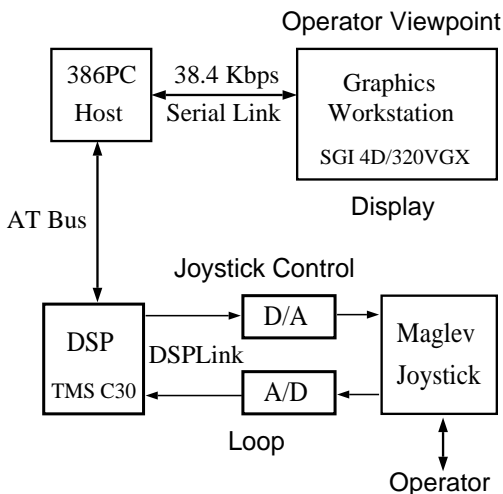


Figure 2 Simulation Block Diagram

An important component of any force reflection system is an active master. A hand controller based on the “Magic

Wrist” [8], uses magnetic levitation to “fly” the handle of the joystick. This removes all mechanical linkages with their backlash and friction. Some additional features of the maglev joystick are programmable stiffness, damping and inertial parameters. It is being used for this research as its excellent backdriveability and force resolution are important. The small workspace of the joystick does introduce complexities when controlling a slave with a large workspace. For the machines being examined, the ratio of master to slave volumes is approximately 1:1000 [14]. Use of a simple scaling factor is not possible, so either position control with indexing or rate control will be used. Most force feedback systems have used position control for stability and a more natural feel, but conventional controls for heavy duty hydraulic machines are all rate controllers.

Coordinated control enables the operator to control the manipulator endpoint in the same frame as his viewpoint. It provides a more intuitive control interface which is easier to learn [12] than the conventional method of individual joint control currently used on hydraulic machines. Coordinated control also provides a better interface for force feedback, as reflected forces can naturally oppose the operators hand motion. The operator to joint space transformation can either be implemented using the inverse kinematics of the manipulator arm or using the inverse Jacobian.

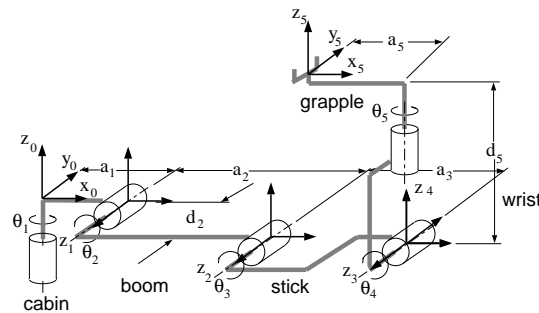


Figure 3 Feller/Buncher Link Schematic

The inverse Jacobian is easier to find for complicated manipulators such as the feller/buncher (Fig. 3) and is better for the direct implementation of rate control. While the Jacobian approach fails at manipulator singularities, these are outside of the workspace of the machine being examined and thus not a problem.

The feller/buncher simulator system was developed using rate control and the inverse Jacobian. A Silicon Graphics Iris provided the real time operator viewpoint from the cabin and reflected the calculated forces and torques at the grapple back to the operator hand. Preliminary results indicated that direct force feedback did not have a very good

feel (the endpoint forces felt out of phase with the command) and tended to go unstable at any feedback gain that was large enough to be felt by the operator. To gain a better understanding of the system, a simple one dimensional system was examined in both position and rate control.

### 3 Force feedback

Force feedback couples the endpoint forces back to command input. As it closes a feedback loop not present in unilateral manipulators, it can have a destabilizing effect on what was previously a stable system. For this analysis, a simple one dimensional model (Fig. 4) will be examined.

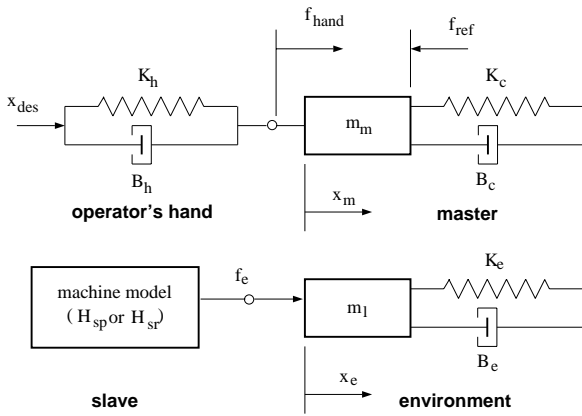


Figure 4 Master/slave system

The coupling between the master and slave depends on the control mode (position or rate) and the feedback mode. The link from master to slave can be described as

$$\begin{aligned} \hat{x}_e &= H_{sp} K_{pos} \hat{x}_m && \text{for position} \\ s \hat{x}_e &= H_{sr} K_{vel} \hat{x}_m && \text{for rate} \end{aligned} \quad (3.1)$$

where  $H_{sp}, H_{sr}$  represent the machine transfer functions for position and rate respectively. A reasonable approximation for  $H_{sp}, H_{sr}$  would be to use a first or second order system with delay (typical joint response delay for hydraulic machines is on the order of 0.4 s). Initial analysis will assume the ideal case,  $H_{sp}, H_{sr} = 1$ .

The motion of the system will depend on which mode the operator controls the master. If  $x_m$  is controlled directly, the endpoint feedback will be felt as a variation of the force applied to the hand. This would eliminate the closed loop stability problem, but would require a rigid hand. The converse case, when the operator controls  $f_{hand}$  directly will result in the feedback information being felt as motion of the master. This eliminates the operator's hand response, but is still not very realistic.

A more complete analysis of the system requires a model of the operator hand. While there exist many complicated models of the human operator which account for sensory delays, motor delays and voluntary control of hand compliance [9], for this initial analysis a simple passive compliance ( $K_h, B_h$ ) will be used [10].

#### 3.1 Position control

To evaluate the stability of a position control manipulator with direct force feedback the following model will be used:

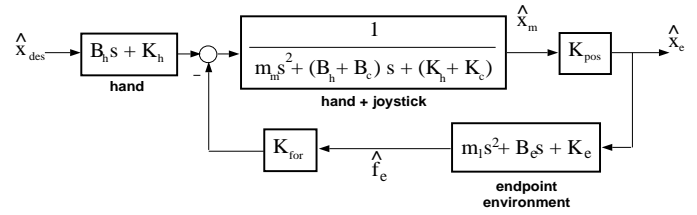


Figure 5 Force feedback with compliant hand

The system transfer function is given by:

$$\frac{\hat{x}_e}{\hat{x}_{des}} = \frac{K_{pos}(B_h s + K_h)}{m' s^2 + B' s + K'} \quad (3.2)$$

where

$$\begin{aligned} m' &\equiv m_m + K_{pos} K_{for} m_l \\ B' &\equiv B_h + B_c + K_{pos} K_{for} B_e \\ K' &\equiv K_h + K_c + K_{pos} K_{for} K_e \end{aligned} \quad (3.3)$$

Examination of the above transfer function indicates that the composite system will act like a simple mass/spring system.

An approach to ensure that the force felt corresponds to the force at the endpoint is to match the joystick impedance to that of the environment.

$$\begin{aligned} f_{hand} &= m_m \ddot{x}_m + B_c \dot{x}_m + K_c x_m \\ f_e &= m_l \ddot{x}_e + B_e \dot{x}_e + K_e x_e \end{aligned} \quad (3.4)$$

With a command transfer function of  $x_e = K_{pos} x_m$  and a force transfer function of  $f_{hand} = K_{for} f_e$  one finds that to maintain a corresponding feel at the master,  $m_m, B_c$  and  $K_c$  need to be adjusted such that

$$\frac{m_m s^2 + B_c s + K_c}{m_l s^2 + B_e s + K_e} = K_{pos} K_{for} \quad (3.5)$$

For flat frequency response, this would require

$$\begin{aligned} m_m &= K_{pos} K_{for} m_l \\ B_c &= K_{pos} K_{for} B_e \\ K_c &= K_{pos} K_{for} K_e \end{aligned} \quad (3.6)$$

While position control is the most natural mode to apply force feedback to, it does require a large master workspace or large position scaling factors. Position control has formed the basis of previous investigations of force feedback on hydraulic machines [3][2].

## 3.2 Rate control

### 3.2.1 Force feedback

Rate control is used in many machine control mechanisms to provide fine control over a large workspace using a limited master control space. However, it introduces complications when used with force feedback. The main source of these complications is the integration of the command signal, which results in the system only being stable when  $x_m$  is zero.

For rate control the block diagram will be similar to Fig. 5, replacing  $K_{pos}$  with  $\frac{1}{s}K_{vel}$ . In this case the transfer function is:

$$\frac{\hat{x}_e}{\hat{x}_{des}} = \frac{K_{vel}(B_h s + K_h)}{m_m s^3 + B^* s^2 + K^* s + K_{vel} K_{for} K_e} \quad (3.7)$$

where

$$\begin{aligned} B^* &\equiv B_h + B_c + K_{vel} K_{for} m_l \\ K^* &\equiv K_h + K_c + K_{vel} K_{for} B_e \end{aligned} \quad (3.8)$$

The system is a degree higher in order than the position case, and the stable values for  $K_{vel} K_{for}$  are restricted to smaller values than the corresponding position case.

Analogous to the impedance matching approach for position control, for the rate control case:

$$\begin{aligned} \hat{f}_e &= [m_l s^2 + B_e s + K_e] \hat{x}_e \\ &= [m_l s^2 + B_e s + K_e] \frac{K_{vel}}{s} \hat{x}_m \\ \hat{f}_{hand} &= [m_m s^2 + B_c s + K_c] \hat{x}_m \end{aligned} \quad (3.9)$$

If the endpoint force is scaled and returned directly ( $\hat{f}_{hand} = K_{for} \hat{f}_e$ ), then an increase in the endpoint load will not be felt as a mass increase but rather as a viscosity increase. In a similar fashion, environmental damping will be felt as a spring force. Rate control with direct force feedback leads to an unnatural feel of the machine load. To maintain similar feel to the position case,  $\hat{f}_{hand} = s K_{for} \hat{f}_e$ , i.e. the derivative of the endpoint force should be returned (after scaling) rather than the force itself. While this will give a more natural feel, it will not provide feedback of constant forces at the endpoint, and thus remove most of the useful information for a contact task.

### 3.2.2 Stiffness feedback

As direct force or force derivative feedback has proved to be unsatisfactory with rate control, a technique where the endpoint force is reflected as a stiffness change of the handcontroller has been examined. The resulting system is nonlinear and difficult to analyze, but provided satisfactory performance in experiments.

By varying the stiffness rather than returning a force to the handle, the system will remain stable for zero input. The joystick is never driven away from its neutral point, as there is always a finite restoring force. As long as the joystick itself is stable, its long term behaviour will be that of an isolated mass/spring/damper combination. A finite deadband extends linear behaviour of the system outside of  $x_m = 0$  and so a finite hand force can be accommodated within the linear region.

The model used in this analysis is the same one used for the linear control schemes (Fig. 4), with  $K_c$  now a function of  $f_e$ . For the master:

$$m_m \ddot{x}_m + B_c \dot{x}_m + K_c(f_e) x_m = f_{hand} \quad (3.10)$$

where

$$f_{hand} = B_h (\dot{x}_{des} - \dot{x}_m) + K_h (x_{des} - x_m) \quad (3.11)$$

and

$$K_c(f_e) = K_{nom} + K_r f_e \quad (3.12)$$

for the simplified case of linear stiffness with no saturation. The slave force  $f_e$  depends on the endpoint environment (Fig. 4)

$$f_e = m_l \ddot{x}_e + B_e \dot{x}_e + K_e x_e \quad (3.13)$$

The endpoint velocity  $\dot{x}_e$  tracks the master position

$$\dot{x}_e = H_{sr} K_{vel} x_m \quad (3.14)$$

where  $H_{sr}$  is the machine transfer function. As above, the ideal case of  $H_{sr} = 1$  will be examined. Substituting (3.12) and (3.13) in to (3.10) yields

$$\begin{aligned} f_{hand} &= f_c + f_{fb} \\ f_c &= m_m \ddot{x}_m + B_c \dot{x}_m + K_{nom} x_m \\ f_{fb} &= K_{vel} K_r \left[ m_l \dot{x}_m x_m + B_e x_m^2 + K_e x_m \int x_m \right] \end{aligned} \quad (3.15)$$

where  $f_{fb}$  is the only nonlinear component. Analysis of this nonlinear system is not trivial, but some intuitive arguments can be made regarding its stability.

A necessary condition for stability of this system is the existence of an equilibrium point. A trivial solution to (3.15) would be  $f_{hand} = 0, x_m = 0$ , however a

more interesting case would be an equilibrium point for  $f_{hand} = \text{const} \neq 0, x_m = \text{const} \neq 0$ . As this would imply  $\ddot{x}_m, \dot{x}_m = 0$  (3.15) can be simplified to

$$K_{nom}x_m + K_{vel}K_r B_e x_m^2 + K_{vel}K_r K_e x_m \int x_m = f_{hand} \quad (3.16)$$

However, with  $x_m \neq 0$  the integral term will not remain constant. As all other terms on the LHS are constant, the sum can not be constant. This implies that  $f_{hand}$  can not be constant and therefore no other equilibrium point exists.

The key factor in that destabilizes the system is the basis of rate control *i.e.* for a nonzero input position, there will be a nonzero output velocity. In order to maintain a stable position of the endpoint, and hence stable forces at the endpoint, the master must possess a deadband:

$$\begin{aligned} \dot{x}_e &= K_{vel}(x_m - x_{db}) & \text{for } |x_m| > x_{db} \\ \dot{x}_e &= 0 & \text{for } |x_m| \leq x_{db} \end{aligned} \quad (3.17)$$

For motion outside of the deadband the force on the operators hand will now be

$$\begin{aligned} f_{hand} &= f_c + K_{vel}K_r f_1 x_m \\ f_1 &= m_l \dot{x}_m + B_e(x_m - x_{db}) + \\ &K_e \int (x_m - x_{db}) dt \end{aligned} \quad (3.18)$$

As long as  $|x_m| > x_{db}$ , the integral term in (3.18) will increase. To maintain a constant force,  $|x_m| \rightarrow x_{db}$ . When the master enters the deadband, endpoint motion will cease and  $f_e$  will remain constant. In this case,  $K_c$  will also be constant, and the joystick motion is reduced to a simple second order linear mass/spring system. Increasing the damping of the wrist will reduce overshoot, though the concepts of critical damping do not apply directly to the non linear system outside of the deadband.

Stability of the stiffness control method can be divided into two parts. For motion of the joystick within the deadband, as the system is just a simple second order system, it will be stable for any  $B_e, K_e > 0$ . Outside of the deadband, it must be shown that the handle will enter the deadband within a finite time for any finite input  $f_{hand}$ . A analytical solution via Lyapunov functions has been attempted, so far without success. However, a numerical simulation has shown that the system will converge to the deadband quite quickly for a wide variety of joystick and environment parameters.

## 4 Machine experiments

To test the effectiveness of the force reflecting scheme developed on the feller/buncher simulator, the maglev joystick and controller were integrated into a CAT 215 excavator outfitted with a grapple for log loading experiments.

This particular machine has been the subject of other research, specifically parallel dynamic simulation [15], complex hydraulic system simulation [16] and various experiments in coordinated control [12]. It has a VME based transputer controller and is instrumented to measure joint angles and hydraulic pressures. The machine required the addition of some form of endpoint force sensing for the force reflection experiments.

### 4.1 Endpoint force sensing

The endpoint forces can either be determined from a dedicated force sensor mounted at the end of the grapple, or derived from the hydraulic pressures. Direct measurement is computational simple and is recommended for optimum resolution/performance [17]. Using the pressure transducers avoids the mechanical complications of an endpoint sensor, but introduces the additional problem of accurately modeling the intervening links.

A single axis load cell was installed between the grapple and the end of the arm in order to provide direct measurement of the endpoint forces in the Z direction. This method avoided the difficulties in machine parameter estimation and was able to give an endpoint force resolution on the order of 10 N (0.1% FS). Unfortunately, it was destroyed by side loading before any experiments could be completed. A multiaxis load cell would have been much more durable, but unfortunately one was not available.

#### 4.1.1 Pressure sensors

Using the machine geometry and the cylinder pressures, the applied torque at the joint can be determined. This torque consists of the dynamic components due to the excavator motion, the dissipative components from friction, and the torques due to the endpoint load. Previous work by Sepehri [16] indicated that friction components were not significant, and so these terms were neglected.

Dynamic joint torques can be determined by a recursive Newton-Euler algorithm [18]. The endpoint forces,  $F_{end}$  follow from:

$$\tau_{dynamics} = D(q)\ddot{q} + C(q, \dot{q})\dot{q} + g(q) \quad (4.19)$$

$$F_{end} \equiv \begin{bmatrix} f_x \\ f_y \\ f_z \\ \tau_x \\ \tau_y \\ \tau_z \end{bmatrix} = \left( J(q)^T \right)^{-1} (\tau_{joint} - \tau_{dynamics}) \quad (4.20)$$

Unfortunately, data was not available to compute  $D(q)$  and  $C(q, \dot{q})$ , so the dynamics were simplified to the quasi-static case  $\tau_{dynamics} = g(q)$  and the static inertial parameters of the main links were estimated.

#### 4.1.2 Link parameter estimation

The parameters to be estimated are the link masses and c.g. locations, as well as the nominal end forces due to the grapple. Further simplification restricted force computation to the RZ plane, so only the two endpoint force components  $f_r$  and  $f_z$  were to be measured.

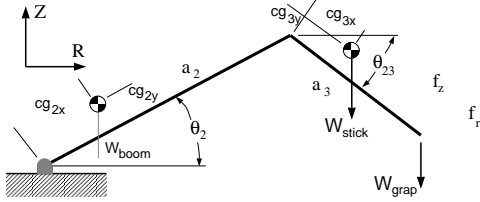


Figure 6 Manipulator Forces

The nominal joint torques due to gravity can be derived quite simply from the geometry.

$$\begin{aligned}\tau_{3_{nom}} &= W_s (cg_{3x} c_{23} - cg_{3y} s_{23}) + W_g a_3 c_{23} \\ \tau_{2_{nom}} &= \tau_{3_{nom}} + W_b (cg_{2x} c_2 - cg_{2y} s_2) + (W_g + W_s) a_2 c_2\end{aligned}\quad (4.21)$$

Rearranging to find the estimateable parameters

$$\mathcal{T}_{joint} \equiv \begin{bmatrix} \tau_{2_{nom}} \\ \tau_{3_{nom}} \end{bmatrix} = \begin{bmatrix} a & b & c & d \\ a & b & 0 & 0 \end{bmatrix} \begin{bmatrix} s_{23} \\ c_{23} \\ s_2 \\ c_2 \end{bmatrix}\quad (4.22)$$

where

$$\begin{aligned}a &= -W_s cg_{3y} \\ b &= W_s cg_{3x} + W_g a_3 \\ c &= -W_b cg_{2y} \\ d &= W_b cg_{2x} + (W_g + W_s) a_2\end{aligned}\quad (4.23)$$

Pressure data for various boom and stick angles was recorded and sorted to obtain static values only, and then converted to the applied joint torque  $\mathcal{T}_{joint}$ . The joint torques and angles were then substituted into (4.22) and the equation solved for  $a, b, c$ , and  $d$  via a least squares fit. Using data from several runs in different parts of the machine workspace resulted in the following estimates.

Parameter	Average Estimate (Nm)	Std. Deviation (Nm)
a	511	763
b	6452	909
c	-7585	1290
d	82729	993

Table 1 Link Parameter Estimates: average of data collected May-June 1992

As one can see, the estimates do not converge very well (the above estimates are based on ~300 data points). Likely sources of error are the unmodeled friction components and pressure transducer errors. Endpoint forces computed using these parameters resulted in errors of 1 to 2 kN over the machine workspace. Of this error, ~600 N could be from the 0.5 % FS error of the pressure transducers. The remainder of the error was probably caused by friction (*i.e.* the initial assumption of negligible friction is not valid in practise).

#### 4.2 Loader experiments.

The endpoint of the loader was controlled in rate mode, with stiffness feedback to the operator. Experiments to evaluate the utility of endpoint force feedback were limited by the poor force resolution and the time lag between the operator command and endpoint movement (on the order of 0.4 s). However, tests were carried out with three subjects to determine roughly the range of forces which could be detected and controlled.

The object of these experiments was simply to determine if it was possible for an operator to perform repeatable application of a desired force, using the joystick stiffness as the feedback mechanism. The experimental procedure consisted of the operator being given a target force between 10 kN in tension to ~15 kN in compression (this range was delimited by the readily available objects). Once given a target force, the operator manoeuvred the endpoint into position (motion was restricted to the vertical axis only). When ready to begin, the operator actuated the start trigger and then moved the endpoint up or down to apply the desired force to the end. Once he had reached the desired force (as determined from joystick stiffness) the stop trigger was actuated, at which point the actual applied force was recorded. The sequence was then repeated for the next target force. Each target force value was repeated three times and the operator was informed after each trial how closely the desired force was achieved to help him correlate stiffness to force.

Results of the complete set of trials are summarized in Figure 7. One can see that the error in the achieved force is relatively constant and approximately equal to the average error in the measurement of the endpoint forces (1 to 2 kN) derived from pressure data. The 95% confidence interval for the force error is from -410 N to 125 N. While the number of trials are small and the errors are quite large, it would appear that it is indeed possible to control the endpoint force using stiffness control, with the largest source of error currently being the poor endpoint force resolution.

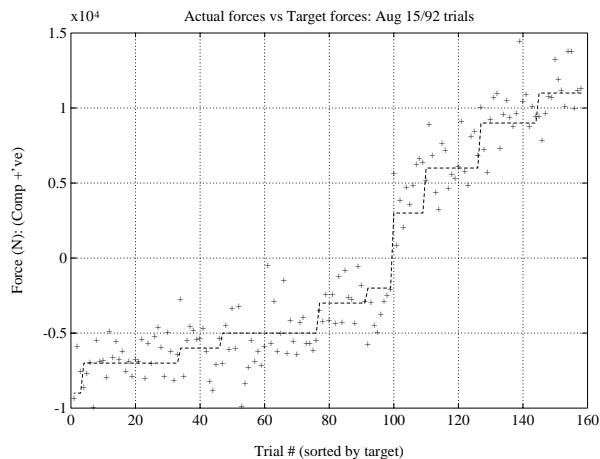


**Figure 7 Endpoint force applied vs. desired force**

## 5 Conclusions

While the goal of a complete force feedback system implemented on a hydraulic machine has not yet been achieved, most of the components have been developed and tested. The maglev joystick has been successfully integrated and tested as a force feedback controller. Coordinated control of complicated machines such as a feller/buncher is easily accomplished using the inverse Jacobian. A novel stiffness control scheme has been developed which utilizes the programmable characteristics of the maglev joystick to implement a force feedback method which works with rate control, enabling small workspace masters to effectively control large workspace slave manipulators.

Problems were encountered in the direct implementation of force feedback were overcome using stiffness control. Endpoint force sensing on a real hydraulic machine proved to be quite a difficult task, as pressure sensors can not provide good force resolution (only 10% of a typical working load). Load sensors directly mounted at the endpoint need to be designed to handle *all* the load components present, not just the ones to be measured. Single axis units are insufficient.

Further work to be completed include mounting a complete system on a machine such as a feller/buncher to test force feedback in multiple axis. Further analysis of the stiffness feedback method is needed to fully understand its capabilities and possible applications. In the future, a complete evaluation of a force feedback system working in the field will be necessary to determine whether this should be implemented on a wider scale.

## References

- [1] D. Stokic, M. Vukobratovic, and D. Hristic, "Implementation of force feedback in manipulation robots," *International Journal of Robotics Research*, vol. 5, pp. 66–76, Spring 1986.
- [2] M. Ostoja-Starzewski and M. J. Skibniewski, "A master-slave manipulator for excavation and construction tasks," *Robotics and Autonomous Systems*, pp. 333–337, 1989.
- [3] R. Langreth, "Smart shovel," *Popular Science*, pp. 82–84, 108–109, 1992.
- [4] E. G. Johnsen and W. R. Corliss, *Human Factors Applications in Teleoperator Design and Operation*. Wiley Series in Human Factors, John Wiley and Sons, 1971.
- [5] G. Burdea and J. Zhuang, "Dextrous telerobotics with force feedback - an overview. part 2: control and implementation," *Robotica*, vol. 9, pp. 291–298, 1991.
- [6] A. K. Bejczy and J. K. S. Jr., "Kinesthetic coupling between operator and remote manipulator," in *Proceedings of the International Computer Technology Conference*, pp. 197–211, American Society of Mechanical Engineers, August 1980.
- [7] S. E. Salcudean, N. Wong, and R. Hollis, "A force-reflecting teleoperation system with magnetically levitated master and wrist," in *Proceedings of the IEEE International Conference on Robotics and Automation*, (Nice, France), May 10-15 1992.
- [8] R. L. Hollis, S. Salcudean, and A. P. Allan, "A six-degree-of-freedom magnetically levitated variable compliance fine-motion wrist: Design, modeling and control," *IEEE Tr. Robotics and Automation*, vol. 7, pp. 320–332, June 1991.
- [9] T. Brooks, "Telerobot response requirements," Tech. Rep. STX/ROB/90-03, STX Robotics, March 1990.
- [10] G. Burdea and J. Zhuang, "Dextrous telerobotics with force feedback - an overview. part 1: human factors," *Robotica*, vol. 9, pp. 171–178, 1991.
- [11] P. D. Lawrence, B. Sauder, U. Wallersteiner, and J. Wilson, "Teleoperation of forest harvesting machines," in *Robotics in Forestry*, (Vaudreuil, Quebec), pp. 36–39, September 1990.
- [12] U. Wallersteiner, P. Stager, and P. Lawrence, "A human factors evaluation of teleoperator hand controllers," in *Proceeding of International Symposium Teleoperation and Control*, pp. 291–296, IFS Ltd., July 1988.
- [13] W. S. Kim, F. Tendick, S. R. Ellis, and L. W. Stark, "A comparison of position and rate control for telemanipulations with consideration of manipulator system dynamics," *IEEE Tr. Robotics and Automation*, vol. RA-3, pp. 426–436, October 1987.
- [14] Caterpillar, June 1984. CAT 215B Sales Literature.
- [15] D. Wong, *Parallel Implementation of Multibody Dynamics for Real-Time Simulation*. PhD thesis, University of British Columbia, May 1991.
- [16] N. Sepeshri, *Dynamic Simulation and Control of Teleoperated Heavy-Duty Hydraulic Manipulators*. PhD thesis, University of British Columbia, September 1990.
- [17] C. H. An, C. G. Atkeson, and J. M. Hollerbach, *Model-Based Control of a Robot Manipulator*, ch. 4. Load Estimation, pp. 65–85. MIT Press, 1988.
- [18] J. Angeles and O. Ma, "An algorithm for the inverse dynamics of n-axis general manipulators using kane's equations," *Computers Math. Applic.*, vol. 17, no. 12, pp. 1545–1561, 1989.